

# Production of perovskite-like $\text{La}_{1-x}\text{Ca}_x\text{MnO}_{3+\delta}$ ferromagnetic thin films by electrochemical reduction

T. MERCER<sup>\*§</sup>, P. A. J. de GROOT<sup>\*</sup>, P. N. BARTLETT<sup>‡</sup>

*Department of Physics\* and Department of Chemistry<sup>‡</sup>, University of Southampton, Highfield, Southampton. SO17 1BJ, Great Britain*

Received 3 December 1996; revised 19 March 1997

Ferromagnetic and perovskite-like thin films ( $<1\ \mu\text{m}$ ) of  $\text{La}_{1-x}\text{Ca}_x\text{MnO}_{3+\delta}$  have been routinely prepared by heat treatment of an amorphous La–Ca–Mn precursor. The precursor was electro-deposited cathodically in the absence of oxygen and water onto polished silver substrates from a nonaqueous solution of the components' nitrates. Analysis by X-ray diffraction and SQUID magnetometry shows these materials exhibit the appropriate structural and magnetic phases indicative of colossal magnetoresistance.

Keywords: *electrochemical deposition,  $\text{La}_{1-x}\text{Ca}_x\text{MnO}_{3+\delta}$  thin films, nanowires, giant magnetoresistance, colossal magnetoresistance, CMR applications*

## 1. Introduction

Colossal magnetoresistance (CMR) in the doped rare earth manganites  $\text{A}_{1-x}\text{B}_x\text{MnO}_{3+\delta}$  has been the subject of intense investigation over the last three years [1–8]. Although sometimes referred to as a large 'giant magnetoresistance' (e.g. [1]), the convention of CMR is adopted throughout this paper for the  $\text{A}_{1-x}\text{B}_x\text{MnO}_{3+\delta}$  magnetoresistive effect. Here A is the trivalent rare earth and B the divalent doping ion that sits on the A site within a perovskite-like structure. While the need for noninduction magnetic sensors (essential for the new generation of high density hard disk drives) is now a major driving force in this interest [9], the huge change in resistivity,  $\rho$ , by application of a magnetic field  $H$  ( $\rho_0/\rho_H \sim 1\ 000\ 000$  has been seen) [6] is fascinating from a purely scientific point of view and is, in itself, worthy of further investigation. Further possible applications, such as memory and magnetic switching devices [10], ensures this will continue. The discovery and definition of CMR ( $\rho_0/\rho_H \geq 1000$ ) [3] in  $\text{La}_{1-x}\text{Ca}_x\text{MnO}_{3+\delta}$  means much attention has focused on that particular system, and hence it is the subject of this paper.

The applications of these materials dictate that thin films or nanowires must be manufactured cost effectively. Current proposed methods of production include molecular beam epitaxy, ion beam sputtering and pulsed laser deposition. Electrochemical deposition (ECD) is an attractive alternative due to the fact that it is carried out in conditions approaching ambient temperature and pressure and that, with such a relatively simple technique, the costs are low. It also negates the need for making/acquiring the bulk targets that the above processes require. A high degree

of control of the structure and thickness of deposited films offers further refinement. Part of the control stems from the way in which the rate of deposition is determined by the current, for example, by altering the charge passed the film thickness can be altered. Furthermore, reproducible deposition of precursors to superconducting films has been achieved within our group by use of this method [11]. One final and highly desirable advantage of ECD is that it can be readily implemented as part of a continuous process. In this paper we report what is believed to be the first production of  $\text{La}_{1-x}\text{Ca}_x\text{MnO}_{3+\delta}$  by cathodic ECD.

## 2. Experimental details

### 2.1. Preparation and electrodeposition

All ECD experiments, including solution preparation, were carried out in an argon filled dry box to exclude oxygen and water. The need for a nonaqueous solution is also apparent here due to the higher reduction potentials of  $\text{La}^{3+}$ ,  $\text{Ca}^{2+}$  and  $\text{Mn}^{2+}$  (–2.37, –2.76 and –1.03 V vs SHE, respectively) compared to that of water (–0.83 V vs SHE) [12]. Dimethylsulfoxide solvent (DMSO) from Aldrich (purity 99.9%) was used as-received but was opened in the dry box to prevent atmospheric water contamination. Nitrate salts of lanthanum, calcium and manganese (Aldrich, purity  $\geq 99.99\%$ ) were stored for not less than one month over phosphorous pentoxide in order to minimize water content.

The electrolyte bath composition was determined empirically from a set of preliminary experiments for a target Ca stoichiometry of  $x = 0$  and  $x = 0.4$  as follows:

<sup>§</sup> Present address of corresponding author: Magnetic Materials Research Group, Department of Physics Astronomy and Mathematics, University of Central Lancashire, Preston, PR1 2HE. UK.

*LaMnO<sub>3+δ</sub> precursor.* 32 mM La(NO<sub>3</sub>)<sub>3</sub> and 8 mM Mn(NO<sub>3</sub>)<sub>2</sub> to give the ratio La<sup>3+</sup>:Mn<sup>2+</sup> of 4:1 in a total 40 mM solution.

*La<sub>0.6</sub>Ca<sub>0.4</sub>MnO<sub>3+δ</sub> precursor.* 48.0 mM La(NO<sub>3</sub>)<sub>3</sub>, 19.2 mM Ca(NO<sub>3</sub>)<sub>2</sub> and 12.8 mM Mn(NO<sub>3</sub>)<sub>2</sub> to give the ratio La<sup>3+</sup>:Ca<sup>2+</sup>:Mn<sup>2+</sup> of 15:6:4 in a total 80 mM solution.

Cathodic ECD was carried out at a constant potential (−3.25 V vs Ag quasi-reference) for 30 min using a standard three electrode arrangement with a 25.0 mm × 12.5 mm counter electrode of 52 mesh platinum gauze (Aldrich, purity 99.90%). Deposition was on a 25.0 mm × 5.0 mm × 0.125 mm silver working electrode (WE) foils (Advent Research Materials, purity 99.97%) that had been previously cleaned and polished using 0.3 μm alumina, distilled water and cotton wool (any residual alumina on the silver foil was removed by a final clean in an ultrasonic bath). The back face of the WE was masked using silicone sealant (Dow Corning, 738 adhesive/sealant) so that deposition occurred on one side only. The three electrodes were suspended vertically in an undivided cell of fixed geometry to ensure their relative positions remained constant for each ECD. The electrolyte temperature was maintained at (29.50 ± 0.1) °C by placing the cell in a ‘dri-block’ heater.

## 2.2. Film composition and crystallization

As-deposited film composition was determined using energy dispersive X-ray spectroscopy (EDS). These amorphous precursor films were crystallized by heat treatment in flowing oxygen at various temperatures and times within the range 700–900 °C and 1–3 h. Cooling for all samples was at 1 °C min<sup>−1</sup>. Film structure was examined by X-ray diffraction using

monochromatic CuK<sub>α</sub> radiation. Magnetization measurements were carried out using a 6 tesla SQUID magnetometer.

## 3. Results and discussion

### 3.1. Film growth and stoichiometry

A plot of the deposition current density, *i*, as a function of time, *t*, is shown in Fig. 1. The smooth plot indicates unperturbed ECD with a profile typical of that expected within a diffusion controlled environment. Indeed, the *i*<sup>−2</sup> ∝ *t* dependency predicted for this by the Cottrell equation [13, 14] was found to hold for short times as shown by the inset of Fig. 1. This implies that the deposition is mass transport controlled. Estimates of the diffusion coefficient, *D*, were obtained from the inset gradient and Cottrell equation and resulted in a value of *D* about 10<sup>−6</sup> cm<sup>2</sup> s<sup>−1</sup> for all samples. The total charge, *Q*, passed during each experiment was determined from the integral of current with time giving values in the range 0.42 C ≤ *Q* ≤ 0.58 C. Assuming perovskite phase densities of 6.72 g cm<sup>−3</sup> for LaMnO<sub>3</sub> and 4.25 g cm<sup>−3</sup> for La<sub>0.6</sub>Ca<sub>0.4</sub>MnO<sub>3</sub>, film thickness estimates of about 700 nm were obtained for both sets from the charge and EDS composition results.

EDS results showed typical La:Mn and La:Ca :Mn ratios of 1.04:1.00 and 0.60:0.42:1.10, respectively, with variations in stoichiometry of not more than 10%, from area to area, over the surface.

### 3.2. Perovskite-like crystal structure

The X-ray diffraction patterns of two representative samples are shown in Fig. 2. Clear perovskite peaks

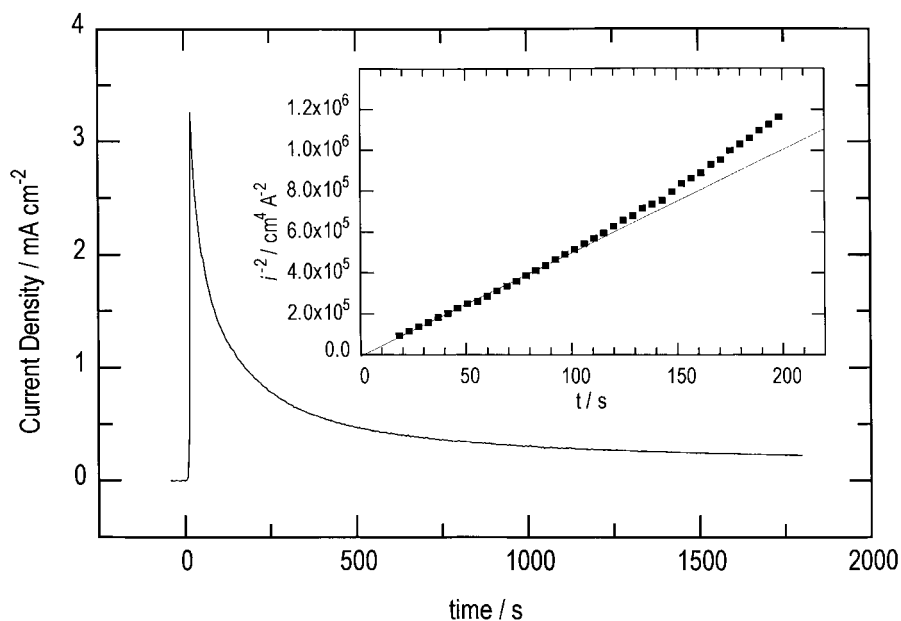


Fig. 1. Typical plot of the current density as a function of time for La–Ca–Mn precursor film. Cathodic ECD was carried out in a dry argon atmosphere at 29.5 °C using a constant potential of −3.25 V (vs Ag quasi-reference). The inset shows the linear relationship between (current density)<sup>−2</sup> and time (first ~tens of seconds) as predicted for an initially diffusion dominant regime.

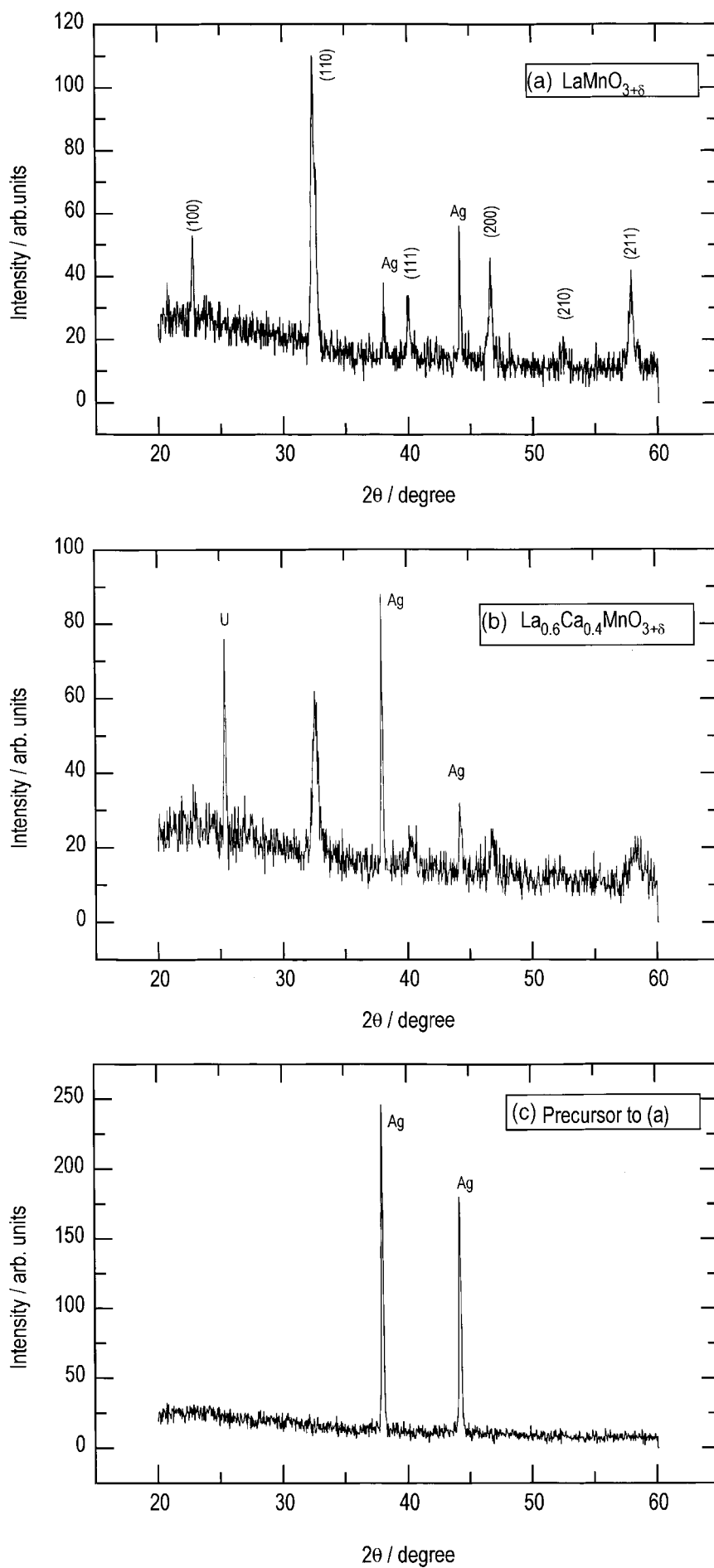


Fig. 2. X-ray spectra of (a)  $\text{LaMnO}_{3+\delta}$  annealed at  $800^\circ\text{C}$  for 2 h and (b)  $\text{La}_{0.6}\text{Ca}_{0.4}\text{MnO}_{3+\delta}$  annealed at  $900^\circ\text{C}$  for 2 h. Both samples were heated in flowing oxygen and cooled at  $1^\circ\text{C min}^{-1}$ . Part (c) shows the X-ray spectra of the amorphous as deposited precursor to (a).

can be seen despite not being able to optimize the radiation beam width of our machine for the small film areas involved (typically  $0.5\text{ cm}^2$ ). The spectra compare well with other samples (e.g. [6]) showing no particular dominance of any  $(h\ k\ l)$  plane and hence indicating a polycrystalline structure. This was further confirmed by contrast with calculated powder diffraction peaks [15]. The lattice parameter,  $a$ , calculated from these patterns ( $(390 \pm 1)\text{ pm}$  for the parent and  $(387 \pm 1)\text{ pm}$  for the doped compound) also compares well quantitatively with the samples of [6] ( $392\text{ pm}$  and  $385\text{ pm}$ , respectively). The reduction in  $a$  with Ca content is expected due to the corresponding increase in  $\text{Mn}^{4+}$  ions at the expense of  $\text{Mn}^{3+}$  ions. As  $\text{Mn}^{4+}$  has a smaller ionic radius ( $52\text{ pm}$ ) as compared with  $\text{Mn}^{3+}$  ( $70\text{ pm}$ ) [16] this leads to an overall smaller lattice parameter. Indeed a calibration between  $a$  and  $\text{Mn}^{4+}$  content [17] shows  $\sim 20\%$  level in the parent ( $x = 0$ ) compound that indicates an excess oxygen content,  $\delta$ , normally as-

sociated with these films when they are annealed in oxygen. The unknown peak U in Fig. 2(b) may be due to a distorted orthorhombic perovskite of  $\text{La}_{1-x}\text{Ca}_x\text{MnO}_{3+\delta}$  as this line is positionally ( $2\theta$ ) within 1% of that found in just such a distorted phase of  $\text{LaMnO}_3$  [18]. This should be investigated further with a full set of samples ( $0 \leq x \leq 1$ ) to see whether or not this is a peculiarity of  $x = 0.4$  in polycrystalline thin films. Heat treatment was always required for crystallization of the precursor films as can also be seen in Fig. 2(c). No peaks were observed in these as-deposited samples which thereby indicates their amorphous nature.

### 3.3. The ferromagnetic signature and its relation to CMR

Magnetization measurements  $M$ , carried out using an applied field of 1 T in the plane of the film, are shown in Fig. 3. With  $M \sim 200\text{ e.m.u. cm}^{-3}$  at 50 K falling to

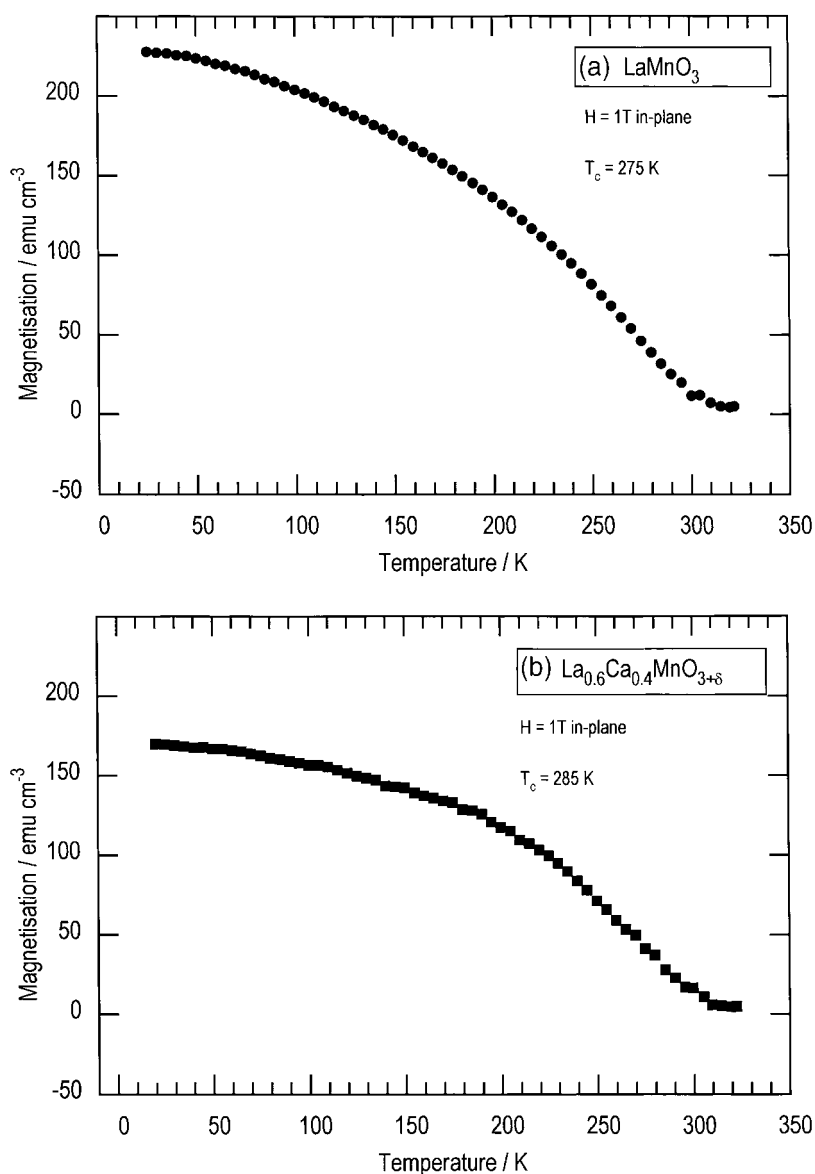


Fig. 3. Magnetization measurements of representative samples of (a), the parent perovskite with a  $T_c$  estimate of  $275\text{ K}$ , and (b) the doped material with  $T_c$  about  $285\text{ K}$ . The broad profile from strongly ferromagnetic down to FM onset at the transition temperature is characteristic of  $\text{La}_{1-x}\text{Ca}_x\text{MnO}_{3+\delta}$  thin films.

a clear transition temperature,  $T_c$ , the films are evidently strongly ferromagnetic (FM) [4]. The broad transition is characteristic of  $\text{La}_{1-x}\text{Ca}_x\text{MnO}_{3+\delta}$  thin films [2 and 3] which, along with the same order  $M$ , gives confidence that the correct magnetic phase has been produced. It should be noted here that although the ideal stoichiometric  $\text{LaMnO}_3$  is an antiferromagnetic (AFM) insulating compound, an excess of oxygen has the same net effect as Ca doping. This means that the necessary number of intrinsic  $\text{Mn}^{3+}$  ions are oxidized in order to maintain charge balance and produce a mixed  $\text{Mn}^{3+}/\text{Mn}^{4+}$  state. Zener's model of double exchange [19] can then be used to explain how the onset of conductivity (due to indirect hole movement between the  $\text{Mn}^{3+}/\text{Mn}^{4+}$  pairs via interstitial oxygen) is inextricably linked with the FM alignment of the Mn moments and thus the onset of the FM state necessary for CMR.  $T_c$  estimates were obtained from the gradient maxima of magnetization against temperature plots and gave values in the range  $270 \text{ K} \leq T_c \leq 285 \text{ K}$ . Similar near room temperature  $T_c$  ( $\sim 275 \text{ K}$ ) has been observed in bulk samples [6], sintered for a period of days in oxygen, as opposed to lower  $T_c$  (in the range 180–220 K) found in as deposited and orientated thin films [2, 8]. However, no significance should be attached to the temperatures found here without a detailed study of polycrystalline thin films over a far greater range of temperatures and times.

#### 4. Conclusions

Precursor films of La–Ca–Mn have been produced by a process of cathodic electrochemical deposition. Heat treatment of these samples has produced  $\text{La}_{1-x}\text{Ca}_x\text{MnO}_{3+\delta}$  thin films of the correct structural and magnetic phases necessary for CMR and hence proves the feasibility of this method as a cheaper and simpler alternative to current techniques such as molecular beam epitaxy and pulsed laser deposition. This is especially so now that epitaxial growth is no longer a prerequisite for large CMR [6, 20]. The technique would require no further processing steps for nanowire deposition (carried out using an electrode masked by commercially available porous ceramic) with the principle already well established for other FM materials [21]. Hence, these results give confidence in its direct applicability, as nanowires allow CMR measurement/use without the need for substrate removal. This last process is required for thin films due to their 'current-in-plane' geometry providing a substrate short circuit path across the material. The 'current-perpendicular-to-plane' arrangement of nanowires negates this problem and means they are currently the main focus of our

attention. Further promising work on a heat treatment method in which an insulating layer is grown between the perovskite and substrate is also being pursued in addition to thick film ( $> 1 \mu\text{m}$ ) removal by use of high temperature adhesive. Results from these studies will be presented in due course.

#### Acknowledgements

The authors would like to thank J. Elliot, R. Langan, K. A. Richardson and G. Goodlet for useful discussion and M. Caplin for producing all the required specialist glassware. Final acknowledgements for assistance with EDS and SQUID magnetometry measurements are reserved for B. A. Cressey and K. Deligiannis respectively. T. Mercer is supported by an EPSRC studentship.

#### References

- [1] R. von Helmolt, J. Wecker, B. Holzapfel, L. Schultz and K. Samwer, *Phys. Rev. Lett.* **71** (1993) 2331.
- [2] K. Chahara, T. Ohno, M. Kasai and Y. Kozono, *Appl. Phys. Lett.* **63** (1993) 1990.
- [3] M. McCormack, S. Jin, T. H. Tiefel, R. M. Fleming and J. M. Phillips, *ibid.* **64** (1994) 3045.
- [4] S. Jin, M. McCormack and T. H. Tiefel, *J. Appl. Phys.* **76** (1994) 6929.
- [5] Y. Tokura, A. Urushibara, Y. Moritomo, T. Arima, A. Asamitsu, G. Kido and N. Furukawa, *J. Phys. Soc. Jpn.* **63** (1994) 3931.
- [6] G. Gong, C. Canedy, G. Xiao, J. Z. Sun, A. Gupta and W. J. Gallagher, *Appl. Phys. Lett.* **67** (1995) 1783.
- [7] R. Mahesh, R. Mahendiran, A. K. Raychaudhuri and C. N. R. Rao, *J. Solid State Chem.* **120** (1995) 204.
- [8] V. A. Vasko, C. A. Nordman, P. A. Kraus, V. S. Achutharaman, A. R. Ruosi and A. M. Goldman, *Appl. Phys. Lett.* **68** (1996) 2571.
- [9] K. Derbyshire and E. Korczynski, *Solid State Technol.* (1995) 57.
- [10] A. Barthelemy, A. Fert, R. Morel and L. Steren, *Physics World* **7** (1994) 34.
- [11] K. A. Richardson, D. M. W. Arrigan, P. A. J. de Groot, P. C. Lanchester and P. N. Bartlett, *Electrochim. Acta.* **41** (1996) 1629.
- [12] CRC 'Handbook of Chemistry and Physics', 63rd edn, CRC Press (1982), Table I, p. D-162.
- [13] A. J. Bard and L. R. Faulkner, 'Electrochemical Methods: Fundamentals and Applications', J. Wiley & Sons (1980), p. 143.
- [14] Southampton Electrochemistry Group, 'Instrumental Methods in Electrochemistry', Ellis Horwood (1990), p. 50.
- [15] 'Lazy-Pulverix', a program originally written by K. Yvon, W. Jeitschko and E. Parthe, *J. Appl. Cryst.* **10** (1977) 73.
- [16] G. H. Jonker and J. H. Van Santen, *Physica* **16** (1950) 337.
- [17] E. O. Wollan and W. C. Koehler, *Phys. Rev.* **100** (1955) 545.
- [18] Joint Council for Powder Diffraction Studies (JCPDS) software database, sheet 35-1353 of PDF-2, sets 1–45.
- [19] C. Zener, *Phys. Rev.* **81** (1951) 403.
- [20] S. Jin, H. M. O'Bryan, T. H. Tiefel, M. McCormack and W. W. Rhodes, *Appl. Phys. Lett.* **66** (1995) 382.
- [21] D. AlMawlawi, N. Coombs and M. Moskovits, *J. Appl. Phys.* **70** (1991) 4421.